# What's really happening on the Barro Colorado Island 50 ha forest plot?

John Alroy[1]

[1]School of Natural Sciences, Macquarie University, NSW 2109, Australia
Email: john.alroy@mq.edu.au

**Abstract**

1. Over the decades, Barro Colorado Island (BCI) has incubated major conceptual and empirical advances in ecology. For example, the theoretical zero-sum multinomial (ZSM), log series, and Poisson log normal (PLN) models have been used to describe abundance distributions and quantify diversity in the BCI 50 ha forest plot.
2. A new model called the compound exponential-geometric series (CEGS) better predicts distributions and quantifies alpha and beta diversity in 1 ha subplots. Distributions are analysed by fitting the four models to each of the subplot's data sets and then predicting counts in adjacent subplots. The PLN performs second-best while the ZSM and log series have almost no predictive power. Meanwhile, only CEGS detects plausible species-area relationships.
3. CEGS assumes nothing specifically about regional speciation rates, density dependence, or competition. It results when recruitment rates are on a per-species basis, whereas death rates are per-capita. It is very much not neutral because it posits that each species has a randomly allocated underlying abundance. It could be interpreted as implying that ecological traits govern demographic rates and in turn structure stem counts. A series of new predictions follows from the model.
4. The model deserves further testing with ecological data, including other forest plot inventories.
5. Synthesis: Ecologists often advocate so-called neutral models in which tree species have identical recruitment and mortality rates, but the actual data for the best-studied tree plot in the world suggest high variation in rates. When a better model is used, internally consistent and sensible species richness estimates are obtained.

## 1 | INTRODUCTION

Community assembly and species diversity are joint problems of key importance in plant and animal ecology. Problematically, undersampling makes it difficult and arguably impossible to infer much about these properties from routine ecological samples enumerating a few hundred individuals (Colwell & Coddington, 1994). A further problem is that recruitment and mortality rates are hard to infer from many animal data sets. For these reasons, a large bulk of literature concerning community patterns has depended on repeat census data for large tropical forest plots (e.g., Plotkin et al., 2000).

The best-known plot of this kind was first censused at Barro Colorado Island in Panama (BCI) in the early 1980s, and it has been continually censused ever since (Hubbell et al., 2024). It remains crucial to ecology because it is the longest-term dataset on stems going down to 1 cm diameter at breast height.

An early and very high-profile debate hinging on BCI erupted in the early part of this century (Matthews & Whittaker, 2014a). Ecologists such as McGill (2003), Connolly et al. (2005, 2009, 2014), Dornelas et al. (2006), and McGill et al. (2006) argued that the log normal distribution of Preston (1948, 1962) was a better model for real data sets – including BCI – than the recently proposed zero-sum multinomial (ZSM) distribution, which was the basis for the famous neutral theory of biodiversity (Hubbell, 1997, 2001). Forceful responses followed (e.g., Volkov et al., 2003), and within a decade many elaborations of the neutral theory had spread throughout the discipline (Rosindell et al., 2011).

To this day, the zero-sum multinomial and its variants are still considered by some to be a good model for the BCI tree data (e.g., May et al., 2016), while the lognormal debate has been termed a "dead end" (Chisholm, 2024). The theory still ramifies even into conservation biology (Buschke, 2021) and palaeontology (Saulsbury et al., 2024). This is despite the fact that ZSM advocates grant the often non-neutral nature of population dynamics in forests, requiring them to extend the model (e.g., Chisholm & O'Dwyer, 2014) in order to "bring theoretical predictions in line with reality" (Chisholm, 2024). Negative density dependence is one early example of such a published mechanism (Volkov et al., 2005). There were already 10 such models within a few years of the ZSM's proposal (McGill et al., 2006).

By contrast, alternatives such as the log normal and log series are fitted without extra theoretical components (e.g., McGill et al., 2003; Connolly et al., 2005, 2009). One could

argue that a theory open to any amount of modification in order to avoid rejection is neither testable nor helpful, but this not to the point of the current fact-based analysis.

Specifically, two important practical observations were lost in the debate. On the one hand, some early comparisons of models depended on simple tests such as binning the data into log units, which has been shown to be somewhat arbitrary and to provide low statistical power (Gray et al., 2006). On the other, more powerful maximum likelihood analyses have rarely been applied to the same data sets using the same equations, in part because advocates of the distributions use different equations (e.g., see Alonso & McKane, 2004; Etienne, 2005; Connolly et al., 2005, 2009).

In this paper, I propose moving past the ZSM vs. log normal debate with respect to BCI by considering a recently published but as-yet quickly evaluated model that is extraordinarily simple and far from a variant of any existing one (Alroy, 2025). It is tested against the ZSM, the log series (LS: Fisher et al., 1943), and the compound Poisson log normal distribution (PLN: Bulmer, 1974) using a consistent and predictive approach. I do not consider alternatives such as the broken stick (MacArthur, 1957) or negative binomial (a.k.a. Poisson gamma) because these have already been dismissed (Connolly et al., 2014; Baldridge et al., 2016) and have few advocates in the realm of BCI researchers.

The implications of fitting these models for understanding species richness are also explored. Many ecologists actually think that richness is far more interesting than hypothetical abundance distributions. However, the problem of estimating it has long been profoundly difficult, with many alternative approaches (Colwell & Coddington, 1994). Indeed, some workers believe it so difficult as to be intractable, fostering an interest in other statistics such as Shannon's $H$ and Simpson's $D$ (e.g., Roswell et al., 2021). The current analysis suggests that local-scale richness can be estimated in an informative and replicable manner with the new formulation.

## 2 | MATERIALS AND METHODS

### 2.1 | Data

The dataset is a 1990 inventory of stems ≥ 1 cm diameter at breast height (DBH) that were found on the 1000 m-wide, 500 m-high 50 ha forest plot on BCI. Censuses at regular intervals have enabled detailed studies of recruitment, turnover, diameter increment, and

many other things (Condit et al., 1995; Muller-Landau & Wright, 2024). A total of 244,003 stems with known species identities and coordinates were inventoried. The data have been made freely available by the Smithsonian Tropical Research Institute (Condit et al., 2024). Although two later censuses are available, the 1990 version with measurements of 1 mm precision was selected to keep the analyses simple. Measurements were rounded to the nearest 5 mm in earlier inventories (Condit et al., 2024).

### 2.2 | The compound exponential-geometric series model

There is a large literature on species abundance models, with many alternatives having been proposed over nearly a century of research (Green & Plotkin, 2007; Matthews & Whittaker, 2014b). Three are prominent in the literature related to BCI: the one-parameter LS (Fisher et al., 1943); the two-parameter PLN (Bulmer, 1974, stemming from Preston, 1948, 1962); and the two-parameter ZSM (Hubbell, 1997, 2001), which incorporates the LS as a special case depending on modelled rates of immigration. The first and last assume that species are equivalent in demographic rates (Kendall, 1948; Hubbell, 1997, 2001), and the LS can even be interpreted as a sampling model that assumes nothing about biological turnover (Fisher et al., 1943). The log normal is non-neutral in assuming that each species has a distinct, randomly drawn underlying abundance. It can derive from a population dynamics model (Engen & Lande, 1996) but could also arise as a random outcome of summing many distinct distributions, following the central limit theorem.

Here I investigate a second non-neutral model that also compounds underlying abundances with a sampling process: exponential or Weibull instead of log normal and geometric instead of Poisson (Alroy, 2025). Note that several other compound distributions are known to ecologists, but all of them assume Poisson sampling (Green & Plotkin, 2007). The compound exponential-geometric series (CEGS) model is derived by assuming that the mean realised count tracks the mean underlying abundance. The mean of the geometric series is $1/p - 1$ where $p$ is the stopping probability in a sampling process. The mean of an exponential is $1/\lambda$ where $\lambda$ is the rate parameter. Given that $\lambda$ itself varies exponentially and notating an exponential random variate as $E$, it follows that:

$$p = \int 1/(E/\lambda + 1)\, \mathrm{d}E \tag{1}$$

λ is therefore the scale parameter of the distribution, analogous to the μ parameter of the PLN. A shape parameter γ analogous to the PLN's σ can be inserted on the right-hand side to increase the variance of the exponential random variate, as in $E^{\gamma}$:

$$p = \int 1/(E^{\gamma}/\lambda + 1)\, dE \quad (2)$$

$E^{\gamma}/\lambda$ is effectively the quantile function of the Weibull distribution. When γ is not equal to 1, CEGS therefore can be called the compound Weibull-geometric distribution, or simply the geometric Weibull (by analogy with "Poisson log normal").

A solution for $p$ can be found with likelihood calculations that consider many candidate values of λ and γ (see below). The probability mass function (PMF) is then found just by plugging eqn. 2 into the standard PMF for a zero-truncated geometric series, which is $(1 - p)^{k-1} p$ where $k$ marks the count classes starting from singletons ($k = 1$). Because the chance of not sampling a species in a geometric series context is just $p$, the resulting species richness estimator is just $S/(1 - p)$ where $S$ is the observed count of species.

### 2.3 | Fitting procedure

Any distribution can be fit in one of three ways: by maximum likelihood, which ignores most of the computable likelihoods across the parameter space; by Bayesian calculations, which require assuming a prior distribution of likelihood probabilities; and by likelihood differencing (LD), which uses the full parameter space and requires no priors. In all such calculations, the simplest likelihood formula is one of the oldest (Alonso & McKane, 2004). If $s_k$ is the species count in each class and $p_k$ is the probability that each count will fall in a given class, the likelihood is just the joint product of $p_k$ raised to the $s_k$ over the range of $k$. Etienne (2005) provided a more complex expression specific to the neutral model, but the simple one is applicable across all models.

LD is computed by (1) setting down an evenly spaced grid of quantiles $Q$ with 51 interior sampling points placed across each dimension; (2) transforming $Q$ into candidate parameter λ or γ values equal to $(-\ln Q)^2$, which yields broad ranges of 0.000377 to 15.612 for each parameter; (3) computing matrices called Δ of absolute values of differences between neighbouring likelihoods running across one parameter dimension or the other; (4) cross-multiplying the two Δ matrices; (5) standardising this product matrix by summation and

division; (6) cross-multiplying the scaled matrix by the logged candidate parameters; and (7) summing and exponentiating to obtain a best estimate of λ or γ. Logging, multiplying, summing, and exponentiating means taking weighted geometric means of candidate values. In practice, it helps to centre the candidate λ matrix after step (2) by dividing it by the geometric mean of the raw counts.

LD works because Δ is near zero in regions where likelihoods are near zero, but by definition high when close to peaks or ridges. It is nearly insensitive to grid spacing because, say, doubling the grid points in only one region cuts the Δ values for that region essentially in half, therefore not changing the net distribution of parameter value weights. Because the grid spacing details have no substantive bearing on the results, there is no sense in which LD assumes a prior distribution.

### 2.4 | Diversity estimates

The PLN and CEGS yield extrapolated diversity estimates in units of species. The LS assumes that richness in the species pool is infinite, which can be confirmed by examining its PMF equation. Claims to the contrary ignore the fact that any legitimate richness estimator must predict a finite number of missing species $s_0$ and the LS probability mass function (Fisher et al., 1943) just doesn't. All the equation ever predicts is the number of species expected to be found in a sample with some number of individuals. However, one form of its governing parameter called α (Fisher et al., 1943) is widely interpreted as a diversity estimator and has strong properties as such. This parameter is literally only a simple function of the observed numbers of species and individuals (Chatfield, 1969). Finally, the zero-sum multinomial has a parameter called θ that tracks α when immigration rates are high and has a similar interpretation (Hubbell, 1997, 2001).

### 2.5 | Software

All of the model PMFs are calculated here using provided R functions. The PLN calculation depends in turn on the *poilogMLE* function in the *poilog* R package (Grøtan & Engen, 2022). The ZSM calculation depends on the *fitmzsm* function in the *sads* package (Prado et al., 2018).

## 2.6 | Simulation analyses

Simulations are used to show whether the observed patterns can be generated with minimally complex but non-neutral population dynamics models. The total species pool size of 400 is matched loosely to the BCI data. Demographic rates vary randomly amongst species, violating neutrality, and are fixed through time. As explained below, because they are balanced the abundances eventually stabilise. And because of the consistent variation, the rates are most easily interpretable as stemming from ecological traits. And because they trade off, this is an *r*/*K* selection model (MacArthur & Wilson, 1967) that also could be termed a fast vs. slow life history model (Saether, 1987; Jeschke & Kokko, 2008).

There are three variants of the model. Death rates always follow a binomial distribution with a death probability $p$. In the first model, recruitment rates follow the geometric series with a stopping probability of $p = 1/(E/0.1 + 1)$ where $E$ is a randomly drawn exponential variate, this expression having the same structure as eqn. 1. The stopping probability $p$ is identical to the death probability for each species. By definition, the expected distribution of recruits across species is just $E/0.1$ because the expected mean outcome of a geometric sampling process is $1/p - 1$.

Population sizes all start at 1 and vary randomly over 1000 time steps. Steady immigration is implicit because the geometric process is not per-capita but per-species (the death probability is per capita). Thus, if a population size reaches zero the species may reappear in following time steps. The simulation therefore assumes that the quadrat is small enough that many of the eventually recruiting propagules have dispersed into it.

The second simulation is very similar except that it assumes a Poisson recruitment process with rates $\lambda$ drawn from $E/0.1$. Because $\lambda$ is the mean expected value of a Poisson draw by definition, the expected recruitment counts again track $E/0.1$.

The third simulation assumes a fixed total population size for all trees on the quadrat. Specifically, there are on average 100 individuals per species, equating to a fixed overall limit of 40,000. The recruitment process is not geometric or Poisson. Instead, the total number of deaths is recorded during each time step and the "spaces" are reallocated randomly among species, with the allocation probability per draw being proportional to $E$.

## 2.7 | Simulation model implications

The simulations make varied assumptions about the birth process, but they share a common structure that predicts how population sizes are governed. Let $q$ be a set of expected per-species recruitment rates regardless of the process and let it be Weibull distributed as $E$ raised to a power $\beta$ and divided by a scaling constant $\kappa$. Let $p$ be the per-capita death probabilities distributed as $1/(E^{\gamma}/\lambda + 1)$ where $\lambda$ is some constant and $\gamma$ is another power. Finally, let $K$ be a list of equilibrium population sizes for the species. Because recruitment and mortality must balance when actual population sizes $N = K$, we know that $q = K\,p$. Therefore:

$$K = q/p = (E^{\beta}/\kappa)\,(E^{\gamma}/\lambda + 1) \tag{3}$$

Now if $E^{\gamma}/\lambda$ is large relative to 1, then approximately:

$$K \sim E^{\beta + \gamma}/(\kappa\,\lambda) \tag{4}$$

$$\ln K \sim (\beta + \gamma)\ln E - \ln(\kappa + \lambda) \tag{5}$$

which is in the form of a linear regression in a log-log space (the entire term after the minus sign is a constant). Note that swapping in the empirical $N$ for $K$ and logged uniform quantiles of the actual non-zero counts for $E$ will not produce a linear pattern because unsampled species will be omitted, throwing off the relationship.

### 2.8 | Empirical tests

All good two-parameter models should be adaptable enough to closely fit a not very large data set, such as a single 1 ha census. Thus, one would discern little by trying to sort things out by computing something like an Akaike information criterion score. The relative performance of the four models is therefore assessed with more a powerful predictive test in which each one is fitted to the data for each 1 ha subplot and the resulting PMF is projected onto the count distributions for all four immediately adjacent subplots. Likelihoods of the counts given the PMFs are computed to assess fit. Strong support for a model is defined as a likelihood ratio of 10 (= 2.303 log units).

A second test is to quantify the relationship between sample size and species diversity, however defined. To do this, accumulation curves are illustrated to show how adding more

and more stems to the examined data set changes the estimates. Expectations differ depending on the sequence in which stems are added. First, stems are added randomly from the overall data set, which should yield flat trends. Second, stems are added starting with those found closest to the southwest corner of the plot, with the ordering being based on the Euclidean distance in metres between each stem's coordinate and this corner. The southwest point was chosen because the coordinates are already recorded relative to it. Diversity should rise with accumulation of stems because of spatial turnover in species composition. Finally, stems are added starting with the physically smallest ones just at the lower sampling limit of 1 cm DBH. Diversity should again be entirely flat because all of the inventoried stems must have reached 1 cm DBH at some point during growth.

## 3 | RESULTS

### 3.1 | Descriptive abundance patterns

Thanks to extremely intense sampling of the BCI plot during 1990, it appears that a large majority of species in the immediate area was captured: there are just 17 singletons out of 303 species. This explains why the BCI data set has been the focus of so much discussion.

Representing the data in a semi-log rank-abundance (RAD) plot (Fig. 1A) suggests that CEGS and the PLN (blue and orange lines) are highly similar. However, using a log-log space shows that the PLN consistently overshoots at high abundances and CEGS is much more accurate (Fig. 1B: putting aside the top two species, the PLN overshoots all the way down to rank 36). Nonetheless, a far more dramatic pattern is the large difference in performance between these two models and the poorly fitting and indistinguishable LS and ZSM (red and purple).

The fact that the ZSM underestimates the abundance of rare species and overestimates that of fairly common ones is actually visible even in early RAD representations of essentially the same data (Hubbell, 1997). It is not a subtle pattern, but key BCI researchers nonetheless favour the ZSM (e.g., Chisholm, 2024). One reason may be that although RADs have a long history in ecology (e.g., MacArthur, 1957; Hubbell, 1997), much of the BCI literature has tested models by examining counts of species binned into categories on a log scale, following Preston (1948: see Hubbell, 1997; McGill, 2003; Volkov et al., 2003; O'Dwyer & Cornell,

2018; Chisholm, 2024). Binning may have obscured the more realistic performance of the log normal.

### 3.2 | Simulation analyses

The BCI abundance distribution (Figs. 1A, B) is roughly matched in its general shape by the simulation (Fig. 2), although the LS and ZSM fall even shorter here when abundances are low. Note again that the lines for these two models overlap completely. CEGS and the PLN again fit most of the counts extremely closely. However, the PLN again overshoots, with the gap being quite visible when the x-axis is logged (Figs. 2B, D, F). There is no consistent gap for CEGS. The results do not depend on whether population sizes are allowed to vary freely and recruitment follows the geometric series (Figs. 2A, B) or Poisson distribution (Figs. 2C, D), or instead if the total population size is fixed at 40,000 and recruitment is binomial (Figs. 2E, F). The important assumptions are that mortality rates are per-capita; recruitment rates are per-species; demographic parameters stem from the exponential distribution in both cases; and the system is open to immigration.

### 3.3 | Predictive tests of abundance

It is potentially problematic that CEGS and the PLN offer superficially similar descriptions of the overall data (Fig. 1A). The predictive analyses at the subplot scale are therefore essential to determine which one is best.

There were 46 west-to-east and 46 east-to-west comparisons (Figs. 3A, B) plus 40 south-to-north and 40 north-to-south comparisons (Figs. 3C, D), for a total of 172. There was usually strong support (likelihood ratio $\geq 10$) for one model against all three of the others considered at once. Specifically, there was uniquely strong support for CEGS in 38 instances, and the only seven contrary cases involved the PLN.

In other words, despite considerable literature premised on the ZSM applying to BCI, the ZSM never prevailed. Indeed, head-to-head comparisons with the ZSM were even more decisive: there was strong support for CEGS in 141 cases and never for the ZSM.

Based on a paired Wilcoxon rank-sum test, the overall comparisons of CEGS to the LS and ZSM tilt greatly in favour of the former ($p \sim 0$), and the PLN comparisons are also significantly different ($p = 0.0007$). The median CEGS negative log likelihood of 650.161 is

better than the others, which are virtually tied: respectively, 652.271, 652.503, and 652.568 for the LS, PLN, and ZSM, equating to substantial likelihood ratios of 8.2, 10.4, and 11.1.

### 3.4 | Diversity accumulation patterns

The methods agree only broadly with respect to variation in diversity across the 50 subplots. CEGS richness estimates are well correlated with PLN estimates (Spearman's rank-order correlation coefficient $\rho = 0.847$, $p \sim 0$). CEGS correlations with $\alpha$ and $\theta$ are much lower ($\rho = 0.223$ and 0.222) and pale in comparison to the nearly perfect match between the latter two diversity measures ($\rho = 0.978$). In essence, $\theta$ presents no new information compared to $\alpha$ – just as their respective fits to the count data are indistinguishable (Fig. 1).

The accumulation curves raise several issues (Fig. 4). Raw richness is mathematically required to rise steadily with accumulation regardless of the treatment and regardless of what is going on biologically (Fig. 4A). Worse, starting with the smallest stems and working up to the largest accumulates species more slowly than drawing stems at random (dotted line in Fig. 4A). This makes little biological sense because all large stems must have passed through the small size classes at some point, so the entire species pool should be available right away. It points to a misleading interplay between size and abundance: small stems of common species initially swamp the sampling pool, so random draws fail to capture enough diversity.

Meanwhile, there is no difference in the rate of accumulation between the fully random data and the accumulation from the southwestern corner of the plot (dashed line in Fig. 4A). The slope of a log-log regression between raw richness and stem count is 0.127 in the former case and 0.133 in the latter. Something is again wrong, because any spatial clumping of conspecific trees should further steepen the spatially concentrated curve.

CEGS shows no such bias (Fig. 4B): it yields nearly the same flat pattern for the random and DBH-based treatments, and it does yield a steeper slope for the coordinate-based accumulations. This point is taken up later.

Fisher's $\alpha$ is problematic (Fig. 4C). It implies a strong decline in diversity as fully random draws continue (thick solid line: slope = –0.047) or as data are drawn from southwest to northeast (dashed line: slope = –0.038). This is biologically impossible because drawing from a larger area must increase the pool of species available for sampling. Furthermore, $\alpha$ again depicts persistently low diversity when stems are drawn from smallest to largest (dotted line) even though all stems of all species must grow through the 10 cm DBH cutoff.

All of these strong and non-biological biases relate to the fact that α governs the log series and the log series assumes an infinite species pool size. In the first two cases, finding few singletons as more stems are encountered therefore causes α to revise itself downward. In the third, uneven counts in small DBH classes obscure overall diversity.

It is highly problematic that α is so lacking in biological signal because α and θ are essentially the same (Fig. 1) and θ is the basis of the neutral model. It is not a coincidence that the log series describes the abundance distribution so poorly (Figs. 1, 3). Thus, the neutral model isn't merely suboptimal for BCI: it is firmly rejected.

Trends for the standard species richness extrapolation index Chao 1 (Chao, 1984) are also illustrated (Fig. 4D) to make two points. First, it essentially does nothing other than mirror the raw richness pattern and add bias and noise (compare with Fig. 4A). Second, CEGS (Fig. 4B) and α (Fig. 4C) disagree strongly with it. Note for example how Chao 1 reverses the relative magnitude of the spatially ordered and size ordered curves (actually lower and higher in the CEGS data). Chao 1 was derived specifically to be a lower bound estimator, but it's still not clear why anyone would feel comfortable with seeing such low values when fully random draws are small, regardless of the protocol. So switching from α to a nominally distribution-free estimator yields no advantage.

Another key question is how the metrics capture the spatial component of beta diversity. This can be assessed in many ways (Anderson et al., 2010), but most simply by looking for increases in diversity estimates as the sampling zone expands from one corner to the whole plot (Fig. 4, dashed lines). Putting aside the unreliable PLN values, the θ values lacking additional information, and the steep first five data points in each curve, CEGS and α positively disagree: a regression of CEGS logged estimates on logged sample size has a slope of 0.047, but the α slope is –0.036. Slopes are much steeper for raw richness (0.120) and Chao 1 (0.130) because of their sensitivity to undersampling.

To put this another way, CEGS picks up beta diversity and Fisher's α does not. Nonetheless, at first glance the 0.043 value seems low because the literature includes many equal or higher slopes for plant ecosystems at comparable scales, such as about 0.25 for five major tropical forest plots including BCI (Plotkin et al., 2000). This compares with the "canonical" predicted slope of 0.262 based on the log normal model of Preston (1962) and with the empirical mean of 0.310 across 90 studies covering many systems that was reported by Connor and McCoy (1979). Although this topic is very complicated for methodological reasons (Connor & McCoy, 1979; Plotkin et al., 2000), it suffices to say that the CEGS slope

actually reflects the known scaling of beta diversity with plot area (Zhang et al., 2017) and that higher slopes in the literature most likely reflect sampling biases in raw species counts (Fig. 4A).

## 4 | DISCUSSION

### 4.1 | Model predictions

Equations 1 – 5 make a series of predictions, and the most relevant is the expression for the equilibribium population size $K$ based on per-species recruitment rates $q$ and per-individual mortality rates $p$ (eqn. 4 in section 2.7). These proposals should be tested in the future using turnover rate data for large plots (e.g., the BCI data of Condit et al., 1995, 2024). They are not the focus here because the first order of business has been to understand a snapshot of abundance and diversity specifically in the BCI plot.

The predictions are:

(1) $q$ and $p$ should either correlate negatively across species or not correlate. This follows from $E$ being the same random variate in all expressions that involve these rates (see section 2.6).
(2) The relationship is unlikely to be linear on any scale because of structural differences in the equations.
(3) Loosely, because $N = K = q/p$ in late succession, as explained previously, abundant species should have high $q$ rates and low $p$ rates. This is definitional, albeit potentially confusing because per-species recruitment and per-species mortality must balance at equilibrium.
(4) If mortality tracks average size, as it usually does around the world (Piponiot et al., 2022), then species with high mean DBH values should numerically dominate late-succession plots (not just in terms of biomass).
(5) The seed and seedling pools should be dominated by species with large adults: total recruitment $q \sim E^{\beta}/\kappa$ is high for them because the per-individual mortality rate $p \sim 1/(E^{\gamma}/\lambda + 1)$ is low as a result of their size, and $E$ brokers a relationship between $q$ and $p$.
(6) As just indicated, the rates should each be distributed folowing as a random exponential variate $E$ raised to some power. The powers and scales may differ between kinds of rates.

(7) If the powers are each 1, then $N \sim K \sim E^2$. If they are not, then $N \sim E^{\beta+\gamma}$ (in line with eqn. 4). In other words, highly variable rates across a plot should yield highly variable adult counts, with the variation being predictable. β and γ can be fitted to actual demographic rates averaged over long time series, so this can be a direct hypothesis test.
(8) The ranked distribution of counts should also approximately follow a ranked exponential random variate raised to a power, i.e., the quantiles of a Weibull distribution (eqn. 4).
(9) A CEGS species abundance distribution should be seen, and it is (Figs. 1 – 3).

It is not directly predicted that:

(1) Species richness will correlate with demographic rates (Phillips et al., 1994). Nothing in the equations implies this.
(2) Plots with high or low turnover will have more or less individuals. This is because the product of scaling constants κ λ in eqn. 4 is arbitrary. The predictions are about individual species, not plots.
(3) Anything in particular will be seen in early succession plots. The model assumes equilibrium.

### 4.2 | Broader implications

Regardless of theoretical strengths and weaknesses, the log series and zero-sum multinomial seem incompatible with the current analysis. They are unable to account for the overall species-abundance distribution (Figs. 1A, B) or any particular case in which a model is fitted to counts for one plot and projected onto the data for an adjacent plot (Fig. 3). It is hard to over-emphasise the fact that their parameters imply negative species-area relationships (Fig. 4C, solid and dashed lines). The general result (Figs. 1A, B, 3) is in accord with some early analyses of the entire plot's distribution (e.g., McGill, 2003), but this fact should not be overinterpreted because very different statistics were used, analyses were descriptive instead of predictive, and CEGS was unknown.

Quite to the contrary, CEGS is a fully plausible model for the empirical data (Figs. 1A, B, 3) and easily generated by simulation (Fig. 2). It presents medium- to low-variance diversity estimates (Fig. 4) that are in true units of species richness. Thus, its values are intuitive and generalisable, as opposed to simply being distribution parameters such as α and θ. It is also

strongly responsive to spatial patterns (dashed line in Fig. 4B) while avoiding an estimation bias related to the overrepresentation of small species in the data set (dotted line in Fig. 4B, as opposed to Figs. 4A, C, D).

Note that CEGS assumes each species has a distinct but fully random underlying abundance and that further variation results from sampling (eqn. 2). This brings up a major point illustrated by the match of the overall count distribution to the simulation: no complex dynamical model is required to generate its pattern (Fig. 2). Here, total recruitment and mortality amounts for each species come into exact balance (eqn. 4), they vary if at all without any net trajectory through time, and there are no ancillary processes such as speciation, density dependence, or competition.

The most important element is actually that death rates are per-capita but recruitment rates are per-species, implying high rates of immigration and therefore quadrat sizes that are small relative to dispersal distances. This assumption is entirely plausible because the average mean seed dispersal distance is 28.7 m at the equator and the average maximum distance is 78.1 m (Chen et al., 2019), so numerous species should be able to disperse seeds hundreds of meters into a 50 ha plot from the edge over a period of decades.

Importantly, the model implies that CEGS should be seen even at large spatial scales because similar equilibrium points (eqn. 4) should be reached everywhere, allowing dispersal rates to track total adult population sizes throughout the larger forest. Indeed, common trees are consistently common across large spatial areas throughout the tropics (Cooper et al., 2024). This surely reflects trait variation that governs tradeoffs in non-neutral demographic rates.

Although other models such as relatives of the PLN (Green & Plotkin, 2007) could be explored in the future, few of the widely-known ones seem plausible (Baldridge et al., 2016). If a superior distribution were to exist, it would be hard pressed to fit the BCI data any better (Figs. 1A, B) and would presumably bear some conceptual and structural relationship to CEGS.

So if the CEGS model is generalisable, the true nature of forest dynamics at BCI and perhaps throughout the tropics is not neutral in the strict sense. Hubbell"s neutral theory of biodiversity has other empirical problems such as predicting implausibly slow extinction rates (Ricklefs, 2006; Chisholm & O'Dwyer, 2014), but the least it could do is fit the BCI data it was originally formulated to explain (Hubbell, 1997). It does not (Figs. 1A, B) – and the same point has been made previously based on very different analyses (McGill, 2003;

May et al., 2016; O'Dwyer & Cornell, 2018). Thus, BCI's dynamics might instead be tied to variation in physical traits that is well-known to govern variation in demographic rates (Iida & Swenson, 2020; He et al., 2022). The empirical and theoretical connections between traits, rates, and the CEGS pattern should be explored in future studies.

**ACKNOWLEDGEMENTS**

I thank Richard Condit, Robin Foster, and Stephen Hubbell for making the BCI data available to the public.

**FUNDING INFORMATION**

The author is the recipient of a Discovery Project Award (project number DP210101324 funded by the Australian Government.

**CONFLICT OF INTEREST STATEMENT**

The author declares no conflicts of interest

**DATA AVAILABILITY STATEMENT**

The data have already been published on Figshare (https://figshare.com/articles/dataset/_Dataset_BCI_50_ha_Forest_Dynamics_Plot_-_1990_Census/25726890?file=46016763).

**REFERENCES**

Alonso, D., & McKane, A. J. (2004). Sampling Hubbell's neutral theory of biodiversity. *Ecology Letters, 10,* 901-910.

Alroy, J. (2025). Does evenness even exist? *Ecology Letters, 28,* e70181.

Anderson, M. J., et al. (2010). Navigating the multiple meanings of b diversity: a roadmap for the practicing ecologist. *Ecology Letters, 14,* 19-28.

Baldridge, E., Harris, D.J., Xiao, X., & White, E.P. (2016). An extensive comparison of species-abundance distribution models. *PeerJ, 4,* e2823.

Bulmer, M. G. (1974). On fitting the Poisson lognormal distribution to species abundance data. *Biometrics,* 30, 651-660.

Buschke, F. T. (2021). Neutral theory reveals the challenge of bending the curve for the post-2020 Global Biodiversity Framework. *Ecology and Evolution, 11,* 13678-13683.

Chatfield, C. (1969). On estimating the parameters of the logarithmic series and negative binomial distributions. *Biometrika, 56,* 411-414.

Chao, A. (1984). Nonparametric estimation of the number of classes in a population. *Scandinavian Journal of Statistics, 11,* 265-270.

Chen, S.-C., Tamme, R., Thomson, F. J., & Moles, A. T. 2019. Seeds tend to disperse further in the tropics. *Ecology Letters, 22,* 954-961.

Chisholm, R. A. (2024). The forests of Barro Colorado Island and the neutral theory of biodiversity. Pp. 337-348 in *The First 100 Years of Research on Barrro Colorado: Plant and Ecosystem Science,* Volume 1. Eds. Muller-Landau, H. C., & Wright, S. J.

Chisholm, R. A., & O'Dwyer, J. P. (2014). Species ages in neutral biodiversity models. *Theoretical Population Biology, 93,* 85-94.

Colwell, R. K., & Coddington, J. A. (1994). Estimating terrestrial biodiversity through extrapolation. *Philophical Transactions of the Royal Society B,* 345, 101-118.

Condit, R., Hubbell, S. P., & Foster, R. B. (1995). Mortality rates of 205 Neotropical tree and shrub species and the impact of a severe drought. *Ecological Monographs, 65,* 419-439.

Condit, R., Hubbell, S., & Foster, R. (2024). BCI 50 ha Forest Dynamics Plot - 2000 census. Smithsonian Tropical Research Institute. Dataset. https://doi.org/10.25573/data.24640098.v1

Connolly, S. R., Hughes, T. P., Bellwood, D. R., & Karlson, R. H. (2005). Community structure of corals and reef fishes at multiple scales. *Science, 309,* 1363-1365.

Connolly, S. R., Dornelas, M., Bellwood, D. R., & Hughes, T. P. (2009). Testing species abundance models: a new bootstrap approach applied to Indo-Pacific coral reefs. *Ecology, 90,* 3138-3149.

Connolly, S. R., et al. (2014). Commonness and rarity in the marine biosphere. *Proceedings of the National Academy of Sciences, USA, 111,* 8524-8529.

Connor, E. F., & McCoy, E. D. (1979). The statistics and biology of the species-area relationship. *American Naturalist, 113,* 791-833.

Cooper, D. L. M., et al. (2024). Consistent patterns of common species across tropical tree communities. *Nature, 625,* 728-734.

Dornelas, M., Connolly, R., & Hughes. T. P. (2006). Coral reef diversity refutes the neutral theory of biodiversity. *Nature, 440,* 80-82.

Engen, S., & Lande, R. (1996). Population dynamic models generating the lognormal species abundance distribution. *Mathematical Biosciences, 132,* 169-183.

Etienne, R. S. (2005). A new sampling model for neutral biodiversity. *Ecology Letters, 8,* 253-260.

Fisher, R. A., Corbet, A. S. & Williams, C. B. (1943). The relation between the number of species and the number of individuals in a random sample of an animal population. *Journal of Animal Ecology,* 12, 42-58.

Gray, J. S., Bjørgesaeter, A., & Ugland, K. I. (2006). On plotting species abundance distributions. *Journal of Animal Ecology, 75,* 752-756.

Green, J. L., & Plotkin, J. B. (2007). A statistical theory for sampling species abundances. *Ecology Letters, 10,* 1037-1045.

Grøtan, V., & Engen, S. (2022). poilog: Poisson lognormal and bivariate Poisson lognormal distribution. R package version 0.4.2.

He, P., et al. (2022). How do functional traits influence tree demographic properties in a subtropical monsoon forest? *Functional Ecology, 36,* 3200-3210.

Hubbell, S. P. (1997). A unified theory of biogeography and relative species abundance and its application to tropical rain forests and coral reefs. *Coral Reefs, 16,* S9-S21.

Hubbell, S. P. (2001). *The Unified Neutral Theory of Biodiversity and Biogeography.* Princeton University Press, Princeton, N. J.

Hubbell, S. P., Foster, R. B., & Rubinoff, I. (2024). Early history of the Barro Colorado Island Forest Dynamics Project. Pp. 47-53 in *The First 100 Years of Research on Barrro Colorado: Plant and Ecosystem Science,* Volume 1. Eds. Muller-Landau, H. C., & Wright, S. J. Smithsonian Institution Scholarly Press, Washington, D. C.

Iida, Y., & Swenson, N. G. (2020). Towards linking species traits to demography and assembly in diverse tree communities: revisiting the importance of size and allocation. *Ecological Research, 35,* 947-966.

Jeschke, J. M., & Kokko, H. (2008). The roles of body size and phylogeny in fast and slow lie histories. *Evolutionary Ecology, 23,* 867-878.

Kendall, D. G. (1948). On some modes of population growth leading to R. A. Fisher's logarithmic series distribution. *Biometrika,* 35, 6-15.

MacArthur, R. H. (1957). On the relative abundance of bird species. *Proceedings of the National Academy of Sciences, USA, 43,* 293-295.

MacArthur, R. H., & Wilson, E. O. (1967). *The Theory of Island Biogeography*. Princeton University Press, Princeton, N. J.

Matthews, T .J., & Whittaker, R. J. (2014a). Neutral theory and the species abundance distribution: recent developments and prospects for unifying niche and neutral perspectives. *Ecology and Evolution, 4,* 2263-2277.

Matthews, T .J., & Whittaker, R. J. (2014b). Fitting and comparing competing models of the species abundance distribution: assessment and prospect. *Frontiers of Biogeography,* 6, 67-82.

May, F., Wiegand, T., Lehmann, S., & Huth, A. (2016). Do abundance distributions and species aggregation correctly predict macroecological biodiversity patterns in tropical forests? *Global Ecology and Biogeography, 25,* 575-585.

McGill, B. J. (2003). A test of the unified neutral theory of biodiversity. *Nature, 422,* 881-884.

McGill, B. J., Maurer, B. A., & Weiser, M. D. (2006). Empirical evaluation of neutral theory. *Ecology, 87,* 1411-1423.

Muller-Landau, H. C., & Wright, S. J., eds. (2024). *The First 100 Years of Research on Barro Colorado: Plant and Ecosystem Science*,Volume 1. Smithsonian Institution Scholarly Press, Washington, D. C.

O'Dwyer, J. P., & Cornell, S. J. (2018). Cross-scale neutral ecology and the maintenance of biodiversity. *Scientific Reports, 8,* 10200.

Piponiot, C., et al. (2022). Distribution of biomass dynamics in relation to tree size in forests around the world. *New Phytologist, 234,* 1664-1677.

Plotkin, J. B., et al. (2010). Predicting species diversity in tropical forests. *Proceedings of the National Academy of Sciences, USA, 97,* 10850-10854.

Prado, P. I., Dantas Miranda, M. & Chalom, A. (2018). sads: maximum likelihood models for species abundance distributions. R package version 0.4.2.

Preston, F. W. (1948). The commonness, and rarity, of species. *Ecology,* 29, 254-283.

Preston, F. W. (1962). The canonical distribution of commonness and rarity. *Ecology, 43,* 184-215, 410-432.

Ricklefs, R. E. (2006). The unified neutral theory of biodiversity: do the numbers add up? *Ecology, 87,* 1424-1431.

Rosindell, J. P., Hubbell, S. P., Etienne, R. S. (2011). The unified neutral theory of biodiversity and biogeography at age ten. *Trends in Ecology & Evolution, 26,* 340-348.

Roswell, M., Dushoff, J., & Winfree, R. (2021). A conceptual guide to measuring species diversity. *Oikos,* 130, 321-338.

Sæther, B.-E. (1987). The influence of body weight on the covariation between reproductive traits in European birds. *Oikos, 48,* 79–88.

Saulsbury, J. G., Parins-Fukuchi, C. T., Wilson, C. J., Reitan, T., & Liow, L. H. (2023). Age-dependent extinction and the neutral theory of biodiversity. *Proceedings of the National Academy of Sciences, USA, 121,* e2307629121.

Volkov, I., Banavar, J. R., Hubbell, S. P., & Maritan, A. (2003). Neutral theory and relative species abundance in ecology. *Nature, 424,* 1035-1037.

Vokov, I., Banavar, J. R., He, F. L., Hubbell, S. P., & Maritan, A. (2005). Density dependence explains tree species abundance and diversity in trropical forests. *Nature, 438,* 658-661.

Zhang, Y., He, F., Loreau, M., Pan, Q., & Han, X. (2017). Scale dependence of the diversity-stability relationship in a temperate grassland. *Journal of Ecology, 106,* 1227-1285.

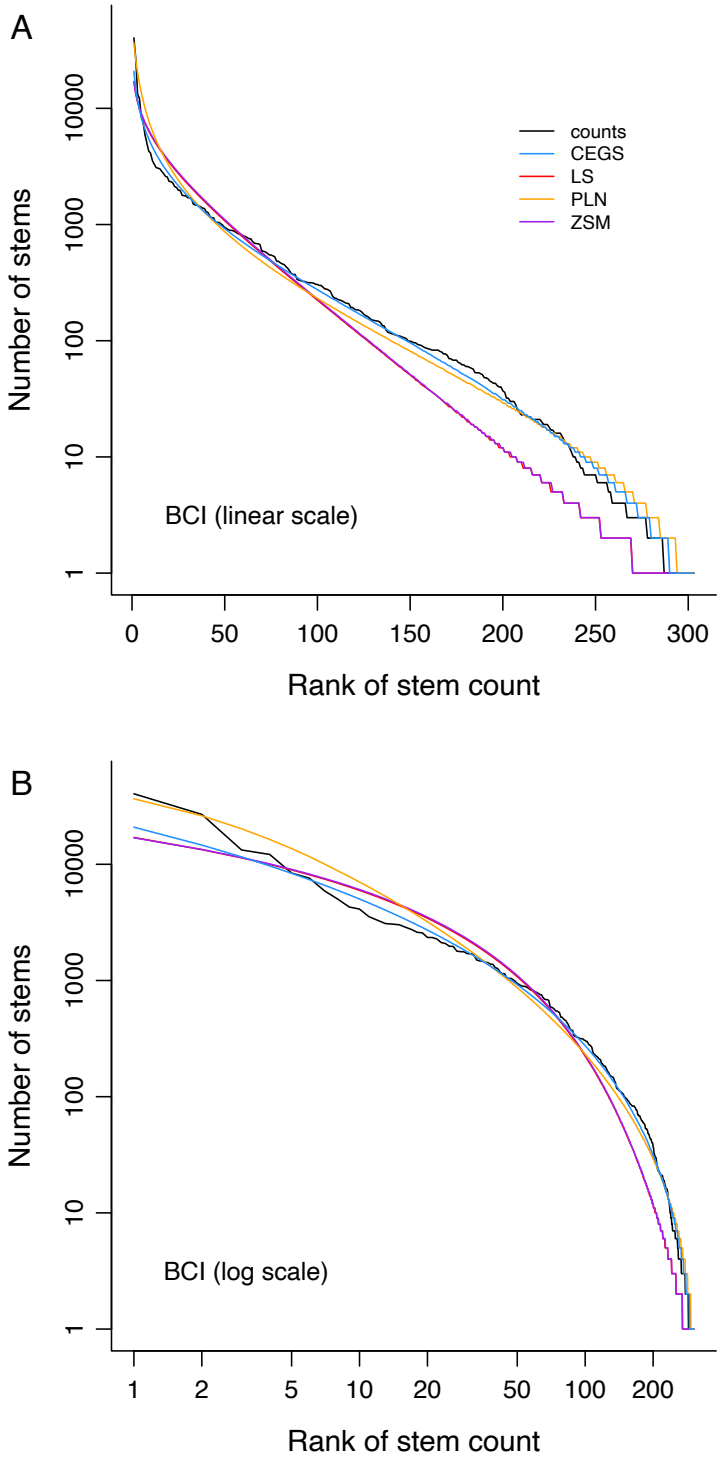


FIGURE 1 | The empirical rank-abundance distribution for the entire Barro Colorado 50 ha plot. Raw counts are in black. Fits are shown for four models: the compound exponential-geometric series (CEGS: blue), log series (LS: red), Poisson log normal (PLN: orange), and zero-sum multinomial (ZSM: purple). x-axes are linear in panel A and log-transformed in panel B.

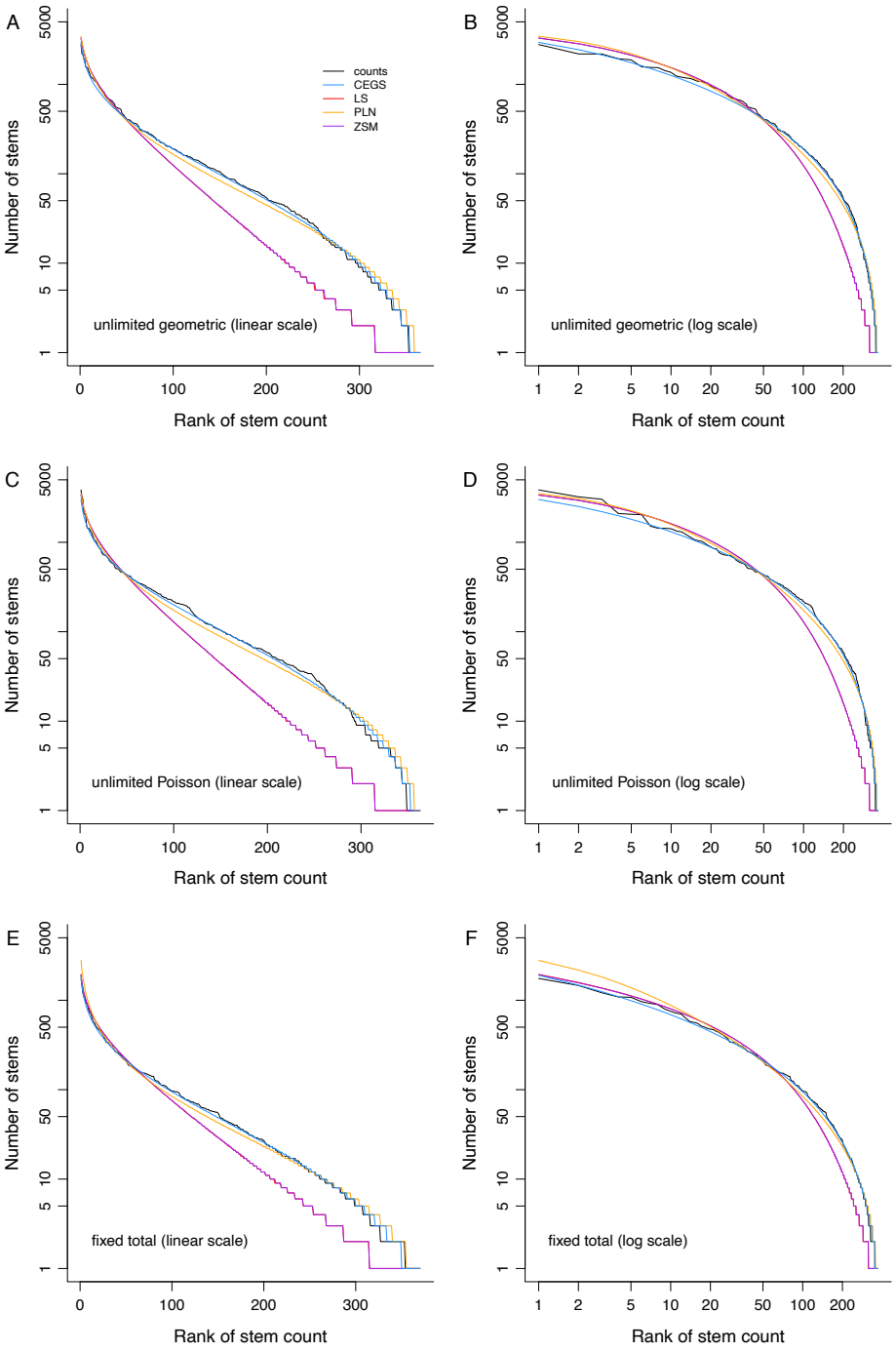


FIGURE 2 | Simulated rank-abundance distributions. Raw counts are in black. Fits are shown for the same models as in Fig. 1. Simulations assume a pool of 400 species and demographic rates that vary among species but are fixed through time. x-axes are linear in panels A, C, and E and log-transformed in panels B, D, and F. (A, B) Population sizes are unconstrained and recruitment counts are distributed geometrically. (C, D) Population sizes are unconstrained and recruitment counts are Poisson distributed. (E, F) The total population size is fixed at 100 x 400 and recruitment is a binomial process.

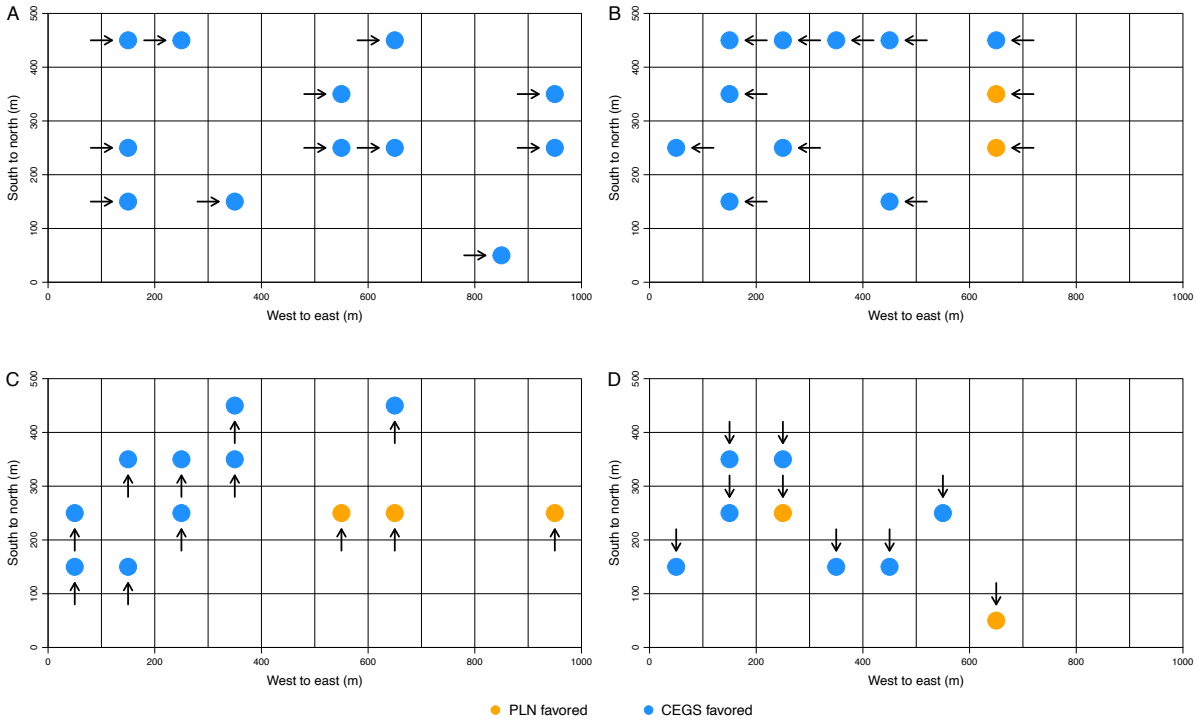


FIGURE 3 | The best abundance distribution model for each 1 ha subplot at BCI based on a predictive test. The four models (Fig. 1) are each fitted to the count data for each subplot and then used to predict counts in plots that are adjacent to the east (A), west (B), north (C), and south (D). The LS and ZSM are never the best model based on a likelihood ratio of ≥ 10. CEGS is best at that margin 38 times (blue points) and the PLN seven times (orange points). Arrows point from subplots where models were fitted to subplots where predictions were tested.

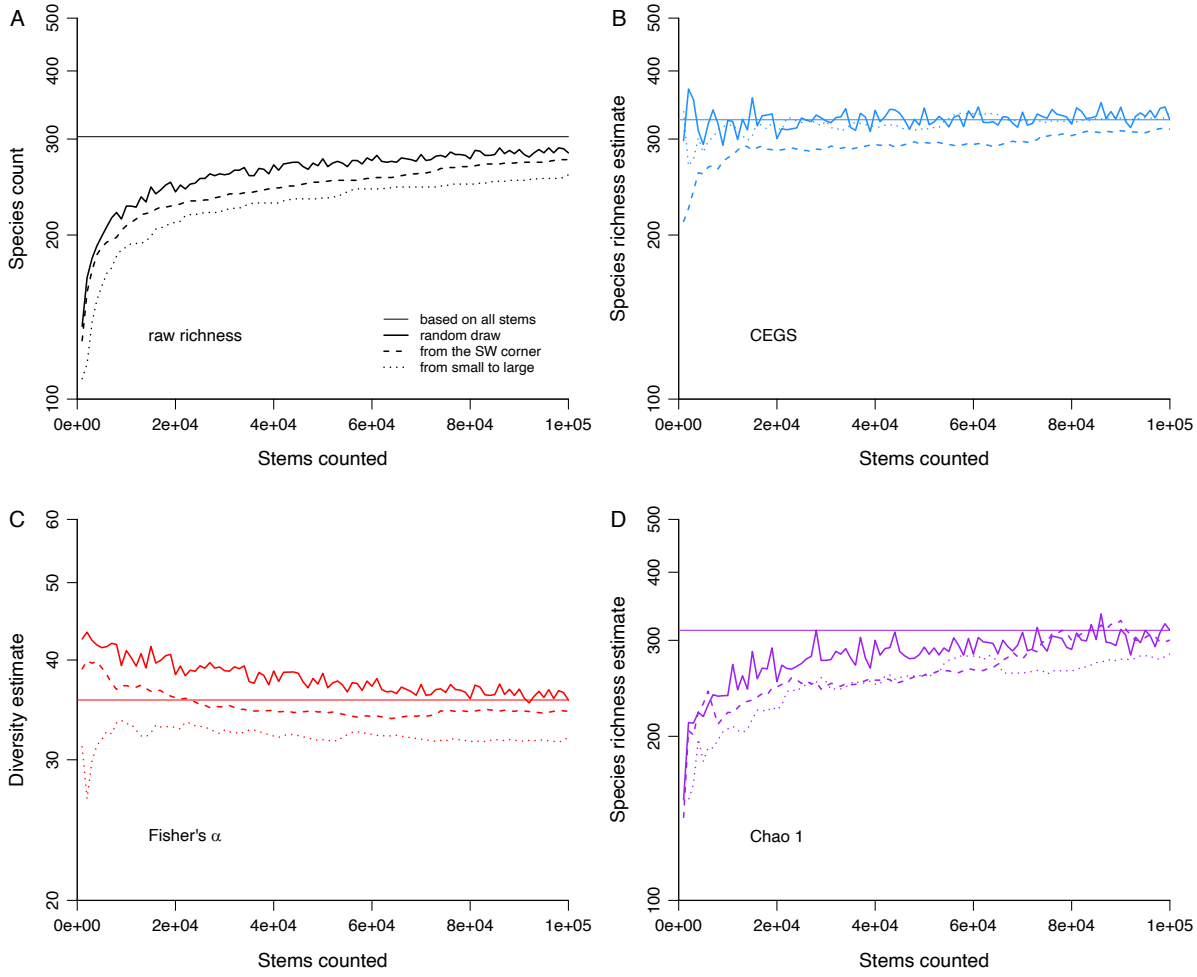


FIGURE 4 | Diversity accumulation curves based on four estimation methods. Three protocols for adding 1000 stems to the examined pool at each of 100 steps are illustrated: stems are randomly and independently drawn at each step (solid lines); stems are drawn in order of Euclidean distance from the southwest corner of the BCI plot (dashed lines); or stems are drawn starting with the smallest ones first in terms of diameter at breast height (dotted lines). Values for the full data set are indicated by thin horizontal lines. y-axes are logged. (A) Raw counts of species. (B) Richness inferred with the CEGS model. (C) Fisher's α (Fisher et al., 1943). (D) Chao 1 (Chao, 1984). PLN data are not depicted due to high variance, while the ZSM's parameter θ is not shown due to its very strong correlation with Fisher's α (Spearman's ρ = 0.978 across the individual subplots illustrated in Fig. 3).